

Optical nanowriting on azobenzene side-chain polymethacrylate thin films by near-field scanning optical microscopy

V. Likodimos,^{a)} M. Labardi, L. Pardi, M. Allegrini, and M. Giordano
INFM and Dipartimento di Fisica "Enrico Fermi," Università di Pisa, Via F. Buonarroti 2,
I-56127 Pisa, Italy

A. Arena and S. Patanè
INFM and Dipartimento di Fisica della Materia e Tecnologie Fisiche Avanzate, Università di Messina,
Salita Sperone 31, I-98166 Messina, Italy

(Received 6 November 2002; accepted 12 March 2003)

Optical writing and subsequent reading of information on thin films of azobenzene side-chain polymethacrylates on the 100-nm scale are demonstrated by near-field scanning optical microscopy (NSOM) with polarization control. Polarized blue light at 488 nm coupled to the NSOM aperture probe activates *trans*–*cis*–*trans* isomerization cycles of the side chains, causing their alignment and thus locally inducing optical birefringence. Red light at 690 nm with modulated polarization is coupled to the same aperture and used to detect optical anisotropy on the local scale. Lines of width on the 100-nm scale were optically inscribed and detected even with no concurrent topographic modification. © 2003 American Institute of Physics. [DOI: 10.1063/1.1572538]

Optical data storage has been the focus of intensive research due to the anticipated superior operation speed and the resulting gain in the inscription of information as well as its noninvasive character. However, the spatial resolution attainable by conventional optical methods is diffraction limited. Near-field scanning optical microscopy (NSOM) has emerged as a promising technique to meet the current demands for high-density optical data storage by circumventing the diffraction limit. Azobenzene-functionalized polymers attract particular interest due their high optical activity producing erasable birefringence gratings,^{1,2} as well as the intriguing photoinduced surface relief phenomenon, which can be readily induced in a single-step process upon exposure of thin films to an interference pattern of polarized light at an absorbing wavelength.^{3,4}

The optical storage mechanism in azobenzene side-chain polymers is based on the isomerization cycles of the azobenzene side-chains between their *trans* and *cis* forms, with respective high and low dipole moments.^{5,6} Polarized light activates *trans*–*cis*–*trans* isomerization cycles, leading statistically to a net realignment of the azobenzene groups perpendicular to the polarization direction, thus locally inducing birefringence. Photoisomerization and the interaction with the optical electric field are also essential for the surface relief formation and the concurrent mass migration that shows a marked polarization dependence,^{7–9} although its microscopic origin is not yet fully understood.¹⁰

NSOM has been previously exploited to detect, with high resolution, the optical anisotropy induced on azobenzene polymers by a pure polarization interference pattern¹¹ as well as to produce subwavelength-sized topographic features relying on the photoinduced surface deformation.^{12–14} All-optical patterning of a photosensitive polymer thin film

was also demonstrated by NSOM with features in the micron range.¹⁵ Submicron all-optical writing and reading was recently obtained by our group on a spin-coated thin film of polymethacrylate (PMA) modified by the insertion in the fourth position of an azobenzene mesogenic unit (3-methyl-4'-pentyloxy) connected to the chain by a hexamethylene spacer (PMA4).¹⁶ Optical structuring was achieved employing NSOM probes with aperture diameter $a \sim 150$ nm. These rather large apertures are a good compromise, providing a localized light source with a well-defined polarization state, as well as higher optical throughput, to implement polarization–modulation detection for the readback process with adequate contrast and signal-to-noise ratio. In this work, we show all-optical writing and reading of features on the 100-nm scale on a thin film of an azobenzene side-chain polymer, realized with polarization–modulation NSOM.

The experiments were performed on a block copolymer of PMA/PMA4 (30/70) deposited as 100-nm thin film on a clean glass substrate by spin coating. The preparation is identical to that previously reported for the PMA4 homopolymer.¹⁷ The copolymer has been introduced because of the higher photosensitivity that is expected with respect to the homopolymer. Despite the higher glass transition temperature T_g of the bulk material ($T_g = 303$ K for the copolymer in comparison with $T_g = 294$ K of the homopolymer), this can be anticipated through the reduction of the nematic potential that tends to destroy photoinduced reorientation.

The NSOM apparatus is based on a homemade instrument,¹⁸ modified with the implementation of polarization–modulation.^{19,20} The beam of a 690-nm laser diode is prepared in a linear polarization state rotating at an angular frequency ω , before being coupled to the NSOM optical fiber (Nanonics Ltd, FN-50). The tip/sample distance is regulated by a tuning-fork-based shear-force detection feedback. Light is collected in transmission by an aspheric lens (NA=0.5) and then detected by a miniaturized photomultiplier tube of extended red sensitivity, after crossing a

^{a)}Current address: Department of Physics, National Technical University, Zografou Campus, 157 80 Athens, Greece; electronic mail: likodimo@gel.demokritos.gr

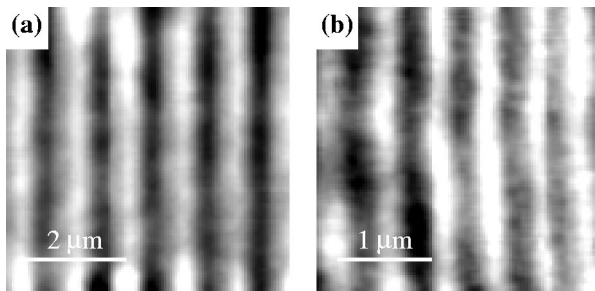


FIG. 1. Birefringence NSOM images ($\lambda = 690$ nm) of optical gratings realized by previously tracing parallel vertical lines with the NSOM probe ($\lambda = 488$ nm) on a thin film of PMA4. The lines are spaced by (a) 1000 nm, and (b) 500 nm.

linear polarizer. In order to improve the sensitivity of the optical channel, an intensity modulation of the laser diode beam at relatively high frequency (~ 25 kHz) has been implemented, followed by a synchronous detection system before the usual polarization modulation detection stage operating at $\omega/2\pi \sim 125$ Hz. This modification allowed to image optical anisotropy features produced with aperture diameters of ~ 100 nm.

The blue line of an Ar^+ laser at 488 nm, controlled in power by an acousto-optic modulator, is used for optical inscription on the polymer surface at ambient conditions. Subsequently, the topographic image is simultaneously acquired with the optical signal averaged over the full polarization-modulation cycle (referred to as DC), as well as the in-phase (X) and quadrature (Y) outputs of the lock-in amplifier that provide the polarization-related signal. Post-processing of the obtained data may then be applied in order to quantify the optical anisotropy.²¹ Defining X_a and Y_a as the values of X and Y recorded on a region that has not been optically modified, the local dichroism C can be estimated as

$$C = [(X - X_a)^2 + (Y - Y_a)^2]^{1/2} / \text{DC}, \quad (1)$$

so that the residual dichroism due to the NSOM optical fiber and aperture can be deconvoluted.

Figure 1 shows optical patterns previously written by tracing vertical lines spaced by 1000 and 500 nm, respectively, with the NSOM tip emitting about 5 nW of laser light at 488 nm (value measured in far field) for the used NSOM probe with $a \sim 150$ nm. The tracing speed was $1 \mu\text{m/s}$, providing a writing fluence of about 5 J/cm^2 . The corresponding topographic relief reveals a rather shallow swelling of the film surface along the inscribed lines of the order of 3 and 2 nm, respectively. These values are much smaller than the surface deformation reported by previous NSOM studies, where longer exposure times and exciting wavelengths close to the absorption maximum, thus increasing both the energy fluence and the mechanical response of the azobenzene polymer, were employed to produce detectable surface reliefs.¹²⁻¹⁴ Repeated experiments with even larger aperture tips and different writing speeds provided direct evidence that the values of light fluence necessary to obtain mass migration are generally much higher than the ones sufficient for changing the local optical properties of the polymer.

Systematic studies of the topography embossing threshold as well as of optical orientation efficiency have been carried out as a function of writing fluence and polarization,

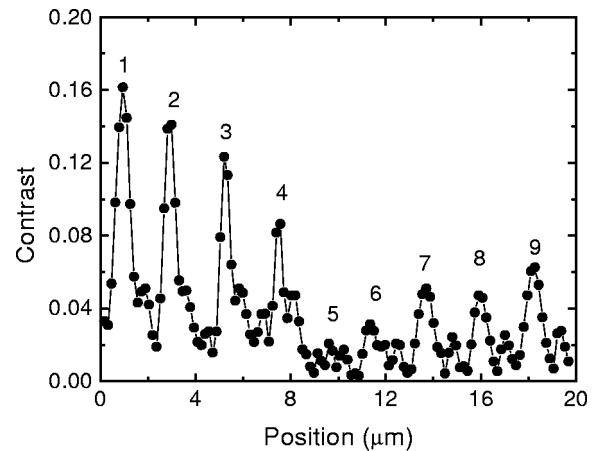


FIG. 2. Processed line profile obtained from birefringence NSOM images of nine vertical lines ($2\text{-}\mu\text{m}$ spaced) imprinted with different scan speeds: from left to right, four lines at 300 nm/s , one line at $10 \mu\text{m/s}$, and four lines at $3 \mu\text{m/s}$.

sample thickness and thermal treatment, and operation temperature. Figure 2 shows a typical processed line profile extracted from a NSOM birefringence image (not shown) recorded after a previous writing of vertical lines with various scanning speeds at 308 K. The presence of a polarization analyzer in the optical path produces an apparent dichroic effect due to the local optical activity of the sample, which has been evaluated using Eq. (1). The corresponding phase variation does not exceed a few degrees. However, determination of the local optical properties in the full near-field regime ($a \leq 50$ nm) releases the assumptions of this analysis and should be addressed by further work.

Figure 3 shows a narrow vertical line obtained with a speed of 30 nm/s , corresponding to a fluence of about 150 J/cm^2 . The imaging quality obtained in this case is limited by the intrinsic resolution of aperture NSOM due to the tip diameter (estimated to be $a \sim 100$ nm in this case), so that the thin line appears with poor contrast and irregular cross section. The full width at half-maximum measured on the profile obtained by averaging all the horizontal scan lines is about 200 nm , while single line profiles show variable thickness from 100 to 200 nm , for example, the one reported in Fig. 3(b) has width of 120 nm . The higher fluence used to produce the narrow line was not yet sufficient to generate any topographic embossing. On the other hand, the optical prop-

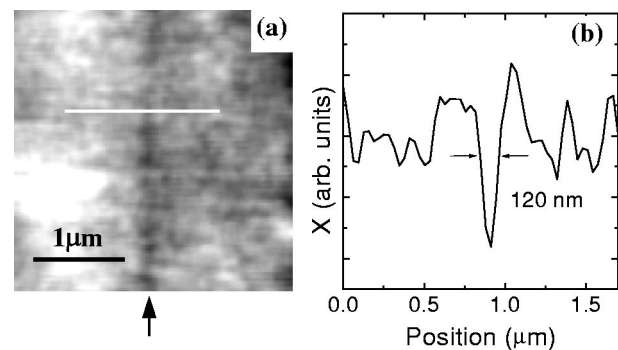


FIG. 3. (a) Birefringence NSOM image ($\lambda = 690$ nm) of a line produced by previous writing with the NSOM probe ($\lambda = 488$ nm) on a thin film of PMA4. The arrow indicates the location of the line. (b) Line profile corresponding to the marked line in (a).

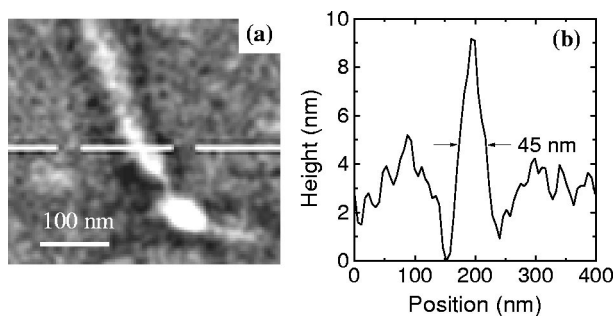


FIG. 4. (a) Topographic shear-force image of a line realized by previous writing with 325-nm laser light coupled to a 50-nm aperture NSOM probe. (b) The line profile at the indicated position in (a) shows a feature width of 45 nm.

erties appear modified on a larger area of several microns around the small feature. This suggests the following picture for the writing process. Near and far fields generated at the NSOM tip are generally characterized by a different intensity and polarization distribution. In particular, the near field is restricted to a spatial region of the order of the aperture diameter also comprising an out-of-plane polarization component due to its nonpropagative character, while the far field is diffracted by the aperture and thus diverges from it. The fraction of near- to far-field electric energy contained in a tiny shell close to the aperture is known to scale as $1/a^2$. Accordingly, the confined near field is able to produce local molecular alignment as well as topographic embossing by increasing the incident fluence. Likewise, the far field emitted by the NSOM probe is able to perform optical alignment, though diffraction limited.

Figure 4 shows an example of topography embossing obtained with 325-nm light, which activates exclusively the *trans-cis* transition and thus favors the main chain rearrangement. Features of 45-nm size have been thus obtained at a scanning speed of 50 nm/s for NSOM probes with $a \sim 50$ nm. The optical throughput of such a tip was enough to enable the writing process by using the highly efficient *trans-cis* transition, but still too low to permit optical readback with the red wavelength.

A point deserving further attention is the role of near and far fields in the readback process. The usual analysis of the NSOM response to anisotropic optical properties is based on considerations valid for propagating fields.²¹ However, the contribution of the near-field interaction becomes particularly important when pursuing higher resolution. Presumably the probing near field is characterized by out-of-plane polarization that will be sensitive mostly to the vertical component of the molecular dipoles. The associated response is then expected to mimic a dichroic rather than a birefringence behavior. Similarly, a component of vertical orientation of the molecules can be induced by both the far- and near-field components of the writing light. However, the emission pattern of the same NSOM tip at different wavelength is expected to be rather different, so that the outcome of the write/

readback process will be in general characterized, as regards both resolution and contrast, by some nontrivial combination of these patterns. The limit case of large probe tips could thus be clear, while the opposite case of extremely small tips needs deeper comprehension since it is the one of interest in order to increase the storage density.

In conclusion, azo-polymethacrylate thin films have been inscribed and read back optically with a resulting line-width of the order of 100 nm using polarization-modulation NSOM. Employment of NSOM probes with smaller aperture and higher throughput will help to assess the ultimate limit for all-optical nanowriting in such materials towards possible applications for ultrahigh density data storage. Further studies to clarify the near-field interaction in both writing and readback processes are necessary to this purpose.

We thank M. Laus for providing the PMA4 polymers and acknowledge MURST for financial support through the project CIPE-P5BW5.

- ¹T. Todorov, L. Nikolova, and N. Tomova, *Appl. Opt.* **23**, 4309 (1984).
- ²R. Wuestneck, J. Stumpe, V. Karageorgieva, L. G. Meier, M. Rutloh, and D. Presher, *Colloids Surf., A* **198–200**, 753 (2002).
- ³P. Rochon, E. Batalla, and A. Natansohn, *Appl. Phys. Lett.* **66**, 136 (1995).
- ⁴D. Y. Kim, S. K. Tripathy, L. Li, and J. Kumar, *Appl. Phys. Lett.* **66**, 1166 (1995).
- ⁵L. Cristofolini, S. Arisi, and M. P. Fontana, *Phys. Rev. Lett.* **85**, 4912 (2000).
- ⁶P. Wu, D. V. G. L. N. Rao, B. R. Kimball, M. Nakashima, and B. S. DeCristofano, *Appl. Phys. Lett.* **78**, 1189 (2001).
- ⁷N. K. Viswanathan, S. Balasumarian, L. Li, S. K. Tripathy, and J. Kumar, *Jpn. J. Appl. Phys.* **38**, 5928 (1999).
- ⁸N. C. R. Holme, L. Nikolova, S. Hvilsted, T. Todorov, P. H. Ramussen, R. H. Berg, and P. S. Ramanujam, *Appl. Phys. Lett.* **74**, 519 (1999).
- ⁹P. Camorani, L. Cristofolini, G. Galli, and M. P. Fontana, *Mol. Cryst. Liq. Cryst.* **375**, 175 (2002).
- ¹⁰J. Kumar, L. Li, X. L. Jiang, D.-Y. Kim, T. S. Lee, and S. Tripathy, *Appl. Phys. Lett.* **72**, 2096 (1998); K. Sumaru, T. Fukuda, T. Kimura, H. Matsuda, and T. Yamanaka, *J. Appl. Phys.* **91**, 3421 (2002), and references therein.
- ¹¹P. S. Ramanujam, N. C. R. Holme, and S. Hvilsted, *Appl. Phys. Lett.* **68**, 1329 (1996).
- ¹²N. Landraud, J. Perett, F. Chaput, G. Lampel, J.-P. Boilot, K. Lahlil, and V. I. Safarov, *Appl. Phys. Lett.* **79**, 4562 (2001).
- ¹³P. S. Ramanujam, N. C. R. Holme, M. Pedersen, and S. Hvilsted, *J. Photochem. Photobiol., A* **145**, 49 (2001).
- ¹⁴S. Patanè, A. Arena, M. Allegrini, L. Andreozzi, M. Faetti, and M. Giordano, *Opt. Commun.* **210**, 37 (2002).
- ¹⁵S. Takahashi, K. Samata, H. Muta, S. Machida, and K. Horie, *Appl. Phys. Lett.* **78**, 13 (2001).
- ¹⁶M. Labardi, N. Coppedè, L. Pardi, M. Allegrini, M. Giordano, S. Patanè, A. Arena, and E. Cefalì, *Mol. Cryst. Liq. Cryst.* (in press).
- ¹⁷A. S. Angeloni, D. Caretti, M. Laus, E. Chiellini, and G. Galli, *J. Polym. Sci., Part A: Polym. Chem.* **29**, 1865 (1991).
- ¹⁸P. G. Gucciaridi, M. Labardi, S. Gennai, F. Lazzeri, and M. Allegrini, *Rev. Sci. Instrum.* **68**, 3088 (1997).
- ¹⁹P. Camorani, M. Labardi, and M. Allegrini, *Mol. Cryst. Liq. Cryst.* **372**, 365 (2001).
- ²⁰L. Ramoino, M. Labardi, N. Maghelli, L. Pardi, M. Allegrini, and S. Patanè, *Rev. Sci. Instrum.* **73**, 2051 (2002).
- ²¹E. B. McDaniel, S. C. McClain, and J. W. P. Hsu, *Appl. Opt.* **37**, 84 (1998); P.-K. Wei, Y.-F. Lin, W. Fann, Y.-Z. Lee, and S.-A. Chen, *Phys. Rev. B* **63**, 045417 (2001).